SUPERSONIC FLOW OVER SHARP-EDGED WINGS

G. P. Voskresenskii, A. S. Il'ina,
and V. S. Tatarenchik

UDC 533.6.011.5

§1. A numerical solution of the problem of steady supersonic flow over sharp-edged wings with shock wave attached to the leading edge was considered in [1]. However, the results presented there refer to wings with a flat upper surface. The present paper gives some results of calculations for wings with curved upper and lower surfaces.

The method, the codes, and the computer solution for the problem are the same as in [1-3]. As was done in these references, the problem was considered in a rectangular coordinate sysem x, y, z with the origin at the leading edge of the wing. The plane $z = 0$ is a plane of symmetry for the wing, and also for the entire flow, since slip is excluded in order to shorten the calculations. The wing surface is given by the function $y = G(x, z)$ and the boundary of the flow region perturbed by the wing is determined by the desired function $y = F(x, z)$.

The problems for the upper and lower surfaces of the wing are considered separately, because the boundary of the perturbed region rests on the wing leading edge. The gasdynamic functions in the perturbed region are determined from the boundary problem for the system of differential equations in partial derivatives (the equations of momentum, continuity, and energy) governing the flow of an inviscid gas. Since the projected components of the sound velocity on the x axis are assumed to be larger than the local sound velocity, the system is hyperbolic in x.

In order to obtain the initial data for the problem the flow over the wing leading edge is calculated on the assumption that the wing has a conical surface and it makes contact with the remaining wing surface in the initial plane $x = x_0$ without discontinuity in the first derivative. A conical flow of this kind is determined by a time-dependent method in terms of similarity of the coordinate x.

The boundary conditions are set up at the wing leading edge and at the boundary of the flow region perturbed by the wing. On the lower wing surface the boundary of the perturbed region corresponds to the shock wave and on the upper surface it corresponds to the shock wave or to the characteristic surface.

At the leading edge an asymptotic approximation to the solution is used, of which the main term corresponds to flow over a wedge washed by a high-speed flow normal to the leading edge at this point. The asymptotic solution differs for the upper and lower parts of the wedge. As a rule, the flow undergoes compression below the wing and expansion above the wedge. In this work we used a joint solution algorithm for both parts of the wing, where the type of boundary conditions at the leading edge corresponded to local values of the approach angle of the external flow velocity to the wing surface.

The determination of the conditions at the outer boundary can be briefly explained as follows. First, conditions are set up for the shock wave. If the difference between the gas pressures ahead of and behind the shock wave is larger than some value ε, then they are considered to have been set up correctly. If this difference is less than ε, then at the given section of the perturbation region the shock wave is regarded as having degenerated into a characteristic surface, which allows the boundary conditions to be simplified.

The problem was solved numerically to second-order accuracy [2, 3] in the regions $x = x_0 + n\Delta x$, with successive transition from one region where the solution has already been found to the adjoining region $x = x_0 + (n + 1)\Delta x$.

For convenience in constructing the algorithm the solution region is normalized by introducing the auxiliary variables

$$t = x;\ \xi = (y - G)/(F - G);\ \theta = z/H(t);\ 0 \leqslant \xi \leqslant 1;\ 0 \leqslant \theta < 1,$$

where $\xi = 0$ is the wing surface; $\xi = 1$ is the boundary of the flow region perturbed by the wing; and H is the z coordinate of the wing leading edge.

Moscow. Translated from Zhurnal Prikladnoi Mekhaniki i Tekhnicheskoi Fiziki, No. 6, pp. 35-42, November-December, 1977. Original article submitted December 3, 1976.

0021-8944/77/1806-0763$07.50

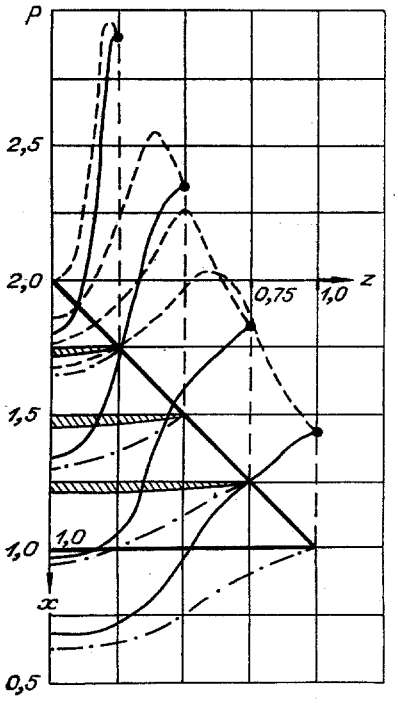

Fig. 1

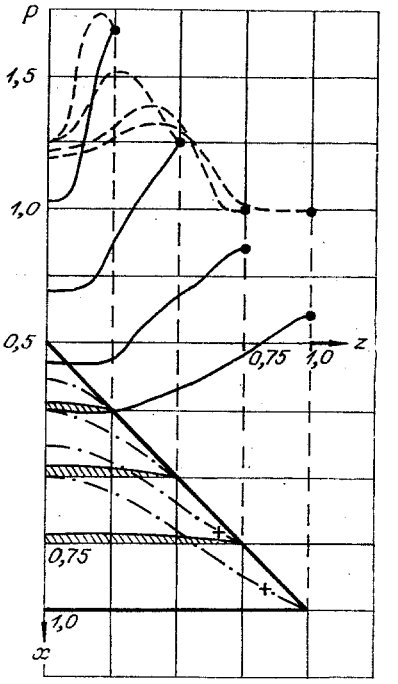

Fig. 2

The mesh in the solution plane has 189 computational points. It is formed from 21 rays with z = const, each having 9 points. The computational step size between the rays is $\Delta\theta = 0.05$, and between the nodes it is $\Delta\xi = 0.125$.

The upper and lower wing surfaces are given by the equation

$$y = G(t, \theta) = 4\bar{c}(1 - \theta^{1+b})t^{1+a}[1 - t - (1 - \theta^{1+e})\mu(t)],$$

where

$$a = \frac{t_0}{1 - t_0}; \quad \mu(t) = \mu_0\left(\frac{t - t_0}{1 - \mu_0 - t_0}\right)^{1+d}.$$

The quantity t_0, which determines the length of the conical nose, was taken to be 0.05, and the coefficients b, e, and d were 0.5, 0.25, and 0.25, respectively. The quantity $\bar{c}$ determines the curvature of the wing surface. For example, for a triangular wing with $a = 0$ the maximum value of the relative curvature in the plane of symmetry is $\bar{c}$. In the examples considered below the values of the coefficients for the upper and lower surfaces are c_u and c_l.

It is assumed that the wing leading and trailing edges lie in the plane y = 0. The leading edge is given by the equation $\theta = 1$ and the trailing edge by the equation $1 - t - (1 - \theta^{1+e})\mu(t) = 0$. Here the previously mentioned coefficient μ_0 determines the sweepback of the trailing edge. For $\mu_0 = 0$ we obtain a wing which has a triangular planform; for $\mu_0 > 0$ it is swept back and for $\mu_0 < 0$ it is rhombic.

For the calculation we chose values of μ_0 for which the trailing edge is supersonic and does not affect the flow within the wing. Since the flow over each wing surface is calculated independently, these surfaces are continued beyond the trailing edge without disturbing the smoothness, and the presence of the trailing edge is not taken into account during the computation. However, the computational results are chosen only from the region lying within the wing contour. Data for the trailing edge can be obtained by interpolating the functions between the rays located before and after the trailing edge.

A special feature of the surface of the wing considered in this paper is a decrease in the relative thickness of the sections at their ends. This surface shape was chosen in order to demonstrate the possibility of obtaining flow with a continuous transition from a compression region to an expansion region, in the area of the leading edge of the top surface.

In the calculations we used dimensionless values of the gasdynamic functions. The pressure and the density were referenced to their values in the oncoming stream and the velocity vector to the quantity $\sqrt{p_\infty/\rho_\infty}$. The linear dimensions were referenced to the wing root chord.

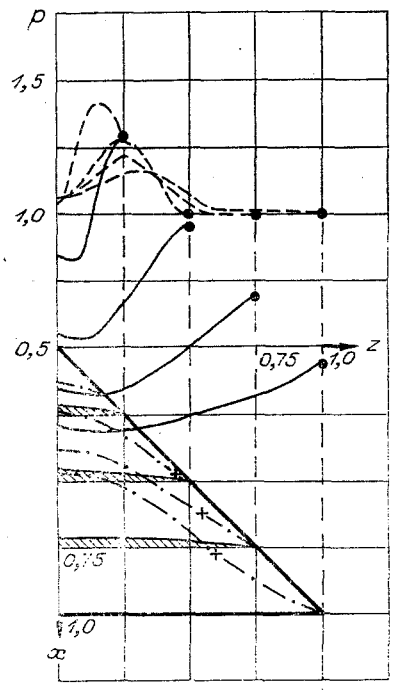

Fig. 3

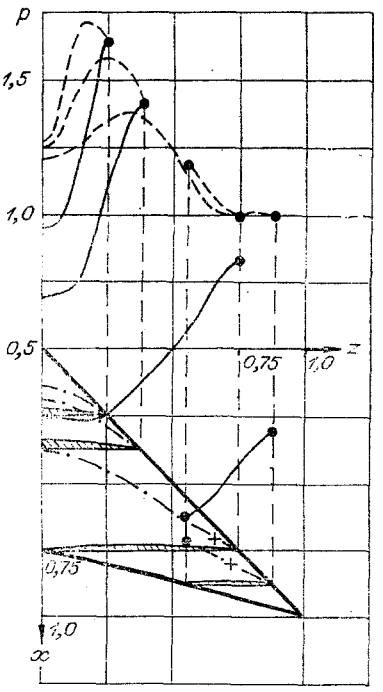

Fig. 4

§2. Calculations of three-dimensional flows by a finite-difference method give a great deal of information on the fields of the gasdynamic functions in the flow region perturbed by the wing, but here we present only some of the typical results.

Figures 1-5 show the pressure distributions at $M_\infty = 3.0$, for the transverse sections x = const, over the wing surface (solid lines) and at the boundary of the perturbed region (dashed line), which may be the shock wave or the characteristic surface. The figures also show the wing contours in plan view and the contours of the transverse sections of the wings. The dot–dash lines show the positions of the perturbed-region boundaries and a cross indicates transition of a shock wave into a characteristic.

The curves in Fig. 1 refer to the lower surface of a triangular wing ($\alpha = 5°$, $\chi = 45°$, $\bar{c}_l = 0.04$, $\mu_0 = 0$); the curves in Figs. 2 and 3 refer to the upper surface of a triangular wing ($\alpha = 5$ and 8°, $\chi = 45°$, $\bar{c}_u = 0.05$, $\mu_0 = 0$); and the curves in Figs. 4 and 5 refer to the upper surface of swept-back and rhombic wings ($\alpha = 5°$, $\chi = 45°$, $\bar{c}_u = 0.05$, $\mu_0 = 0.25$).

For all the wings the pressure distribution curves in the transverse section, for both the lower and the upper wing surfaces, show that the least pressure occurs in the leading-edge section, located immediately behind the conical nose. This is due to the shape of the wing surface, for which the smallest slope lies just behind the conical nose.

For all the wings the curves of pressure distribution behind the shock wave are characterized by the fact that there is a region of pressure drop at the wing leading edge. This increases with increasing distance from the wing nose. It is associated with the presence of a knee in the shape of the shock wave section, e.g., for the lower wing surface it can be clearly seen at x = 0.75 and 1.0 (see Fig. 1). This is apparently due to the fact that the relative thickness of the wing reduces strongly at its ends.

While there is always a flow expansion and the nature of the flow is determined only by the angle of attack for wings of flat plate type (above the upper surface), at a nonzero angle of attack the nature of the flow for contoured wings is determined not only by the angle of attack, but also by the local slope of the plane tangent to the wing surface. Therefore, at a given angle of attack, depending on the shape of the profile, above the upper surface there may be either compression flow or expansion flow, or there may be both, with a continuous transition from a compression region to an expansion region.

This is confirmed by Figs. 2-5, where the slope of the surface tangent to the curve F = F(x, z) is compared with the slope tangent to the section of the characteristic surface at x = 0.75 and 1.0, for flow over the upper surfaces of different wings. The comparison showed that there is little difference. The curves p = p(0.75, z) and p(1, z) for $\xi = 1$ also show that for z > 0.7 the shock wave is almost no different from the char-

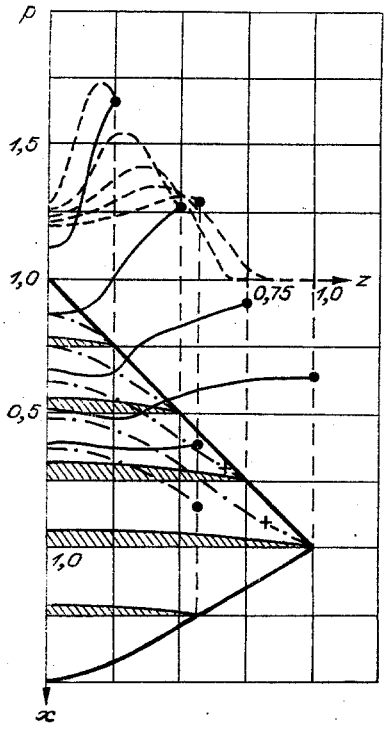

Fig. 5

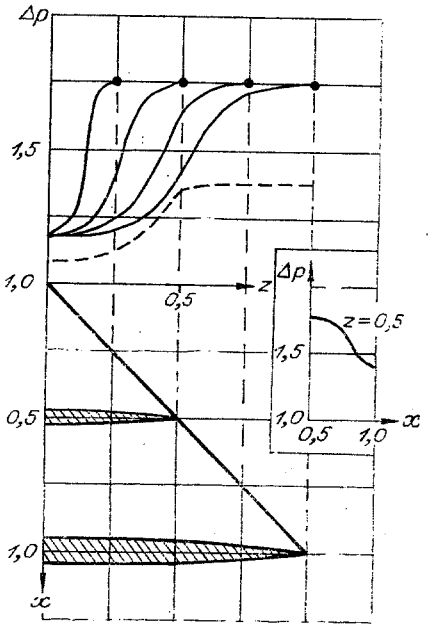

Fig. 6

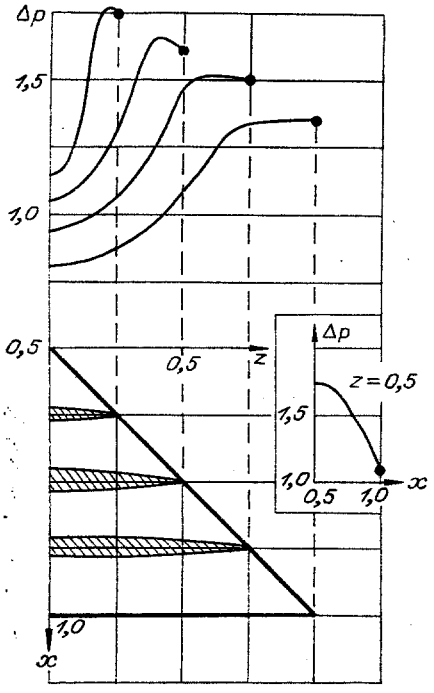

Fig. 7

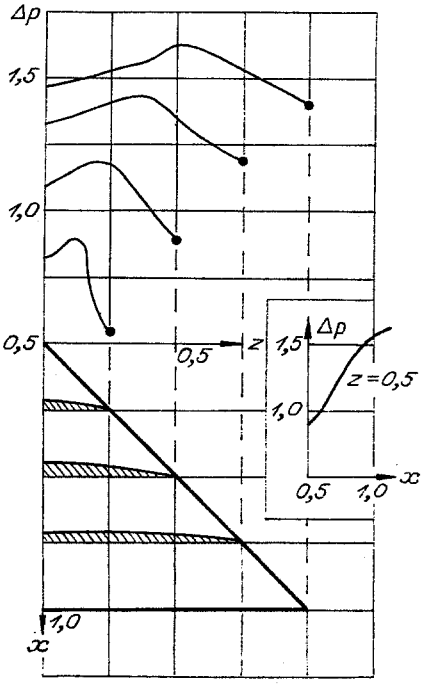

Fig. 8

acteristic surface, except for the fact that at the wing leading edge there is a difference in pressure on the body and in the wave, and therefore there is a flow expansion region at the end of the wing.

The knee point in the shock wave contour at x = 0.75 and 1.0 also occurs for the upper surface, since the pressure distribution for it is the same as for the lower surface.

A comparison of the computed data for flow over a triangular wing at $\alpha = 5$ and 8° (see Figs. 2 and 3) shows us how the gasdynamic functions vary with angle of attack. No other peculiarities in the distribution of the functions were observed for a change of angle of attack. There is a natural general increase in pres-

sure on the lower surface of the wing and a decrease on the upper surface. The "decay" of the shock wave into a characteristic surface above the upper surface of the wing for $\alpha = 8°$ occurs at $z \approx 0.5$, which is somewhat less than the value of z for $\alpha = 5°$.

Calculations of the flow over a triangular wing with the same surface shape but with a different sweepback angle $\chi = 60°$ and a different Mach number $M_\infty = 4.0$ also showed that the above-mentioned features in the pressure distribution and shock-wave shape were also found at this flow condition.

Figures 6-8 show the distribution of pressure difference $\Delta p = \bar{p}_l - \bar{p}_u$ over triangular wings with leading edge sweepback of $\chi = 45°$ at angle of attack $\alpha = 8°$ and $M_\infty = 3.0$. The solid curves in Fig. 6 correspond to a wing with a conical surface ($\bar{c}_u = 0.05$, $\bar{c}_l = 0.03$), and the dashed curve shows the pressure distribution of Δp for a triangular plate with the same sweepback at $x = 1$ ($\bar{c}_u = \bar{c}_l = 0$). Figure 7 shows the pressure difference over a wing of biconvex profile ($\bar{c}_u = 0.05$, $c_l = 0.03$), and Fig. 8 shows the distribution over a wing with a planoconvex profile ($\bar{c}_u = 0.05$, $\bar{c}_l = 0$). The data for the flat surface of this wing and for the triangular plate are taken from [1].

Figures 6-8 also show the pressure difference along the chord $z = 0.5$. It can be seen that the loading distributions are similar for the conical wing and the biconvex wing, but it is different for the planoconvex wing. At $z = 0.5$ the loading decreases with increase in x for the biconvex wing, while it increases for the planoconvex wing. This result cannot be explained, evidently, by the effect of curvature of the mean surface alone. For example, a wing with a planoconvex profile $\bar{c}_u = 0.02$, $\bar{c}_l = 0$ at $\alpha > 0$ will have the derivative $d\Delta p/dx > 0$ in the plane of symmetry, while the wing considered above with a biconvex profile and the same curvature of its mean surface has $d\Delta p/dx < 0$.

Hence, it follows that conclusions regarding the aerodynamic properties of triangular wings in a supersonic flow with a shock wave attached to the leading edge, based only on the nature of the change of the mean surface, may be in error. It is necessary to take into account the nature of the variation of the top surface and especially the lower surface of the wing.

During computation of the flow over the two wing surfaces the aerodynamic coefficients C_t, C_n, and m_z were also evaluated. The coefficients C_t and C_n were calculated in a wing-fixed coordinate system. The coefficient m_z was computed relative to the wing apex and referenced to its root chord. The coefficients C_n and m_z were calculated for the two surfaces, on the assumption that the pressure is zero on the other side.

TABLE 1

M_∞	3	3	3	3	3	3	3	4	3
$\alpha°$	0	0	0	5	5	5	8	5	5
$\chi°$	45	45	45	45	45	45	45	60	45
μ_0	0,00	0,25	−0,5	0,00	0,25	−0,5	0,00	0,00	0,00
Lower surface									
$\bar{c}_l$	0,05	0,05	0,05	0,04	0,04	0,04	0,03	0,02	0,00
C_t	0,0068	0,0069	0,0060	0,0058	0,0067	0,0057	0,0039	0,0013	0,0000
C_n				0,2387	0,2374	0,2354	0,2937	0,1451	0,2305
m_z				0,1450	0,1655	0,1194	0,1746	0,0909	0,1535
Upper surface									
$\bar{c}_u$	0,05	0,05	0,05	0,05	0,05	0,05	0,05	0,05	0,05
C_t	0,0068	0,0069	0,0060	0,0048	0,0054	0,0044	0,0039	0,0032	0,0048
C_n				0,1138	0,1126	0,1133	0,0880	0,0587	0,1138
m_z				0,0656	0,0745	0,0547	0,0500	0,0322	0,0656
Complete wing									
C_t	0,0136	0,0138	0,0120	0,0106	0,0121	0,0101	0,0078	0,0045	0,0048
C_n				0,1249	0,1248	0,1221	0,2057	0,0864	0,1167
				0,124	0,127	0,123			
m_z				0,0794	0,0910	0,0647	0,1246	0,0587	0,0879
x_f				0,615	0,74	0,50			
				0,67	0,78	0,55			

The aerodynamic coefficients C_t and C_n in the body-fixed coordinate system can be recalculated as coefficients C_x and C_y in the velocity coordinate system, as is known, using the formulas

$$C_x = C_n \sin \alpha + C_t \cos \alpha, \; C_y = C_n \cos \alpha - C_t \sin \alpha,$$

but the coefficient m_z remains unchanged.

Table 1 shows values of the coefficients C_t, C_n, and m_z both for the separate wing surfaces and as a total for the entire wing. The coefficient C_t for the total wing was obtained by adding the coefficients for the upper and lower wing surfaces, while the coefficients C_n and m_z were obtained from the difference in the coefficients for the upper and lower wing surfaces.

The last column of Table 1 shows the location of the aerodynamic focus with respect to angle of attack, i.e., the point of application of the increment of wing lift force during a small change of angle of attack. Since the profile of the wings considered is asymmetrical, the focus does not coincide with the center of pressure, which is the point of application of the total lift force. To determine the position of the focus supplementary calculations were made of flow over a wing at $\alpha \pm 0.5°$. The focus was determined relative to the wing nose as a fraction of the root chord.

For the parameters $M_\infty = 3.0$, $\alpha = 5°$, and $\chi = 45°$, Table 1 shows the values of C_n and the focus x_f of flat wings of the same planform as the curved wing. These data were obtained from reference [1], and are printed below the corresponding values of the coefficients C_n and x_f of the curved wing.

To verify the calculations we compared values of the Bernoulli integral in the incident stream with its values in regions perturbed by the presence of the wing. The difference in these values did not exceed 1% for individual cases and was mainly less than this.

More complete results of the calculations for the upper and lower halves of the flow are given in [4], which tabulates the position of the perturbed region boundary, the velocity components, the pressure, and the density at 55 points in 4 cross sections for a triangular and a swept-back wing. For the rhombic wing tables are given for 5 cross sections.

LITERATURE CITED

1. G. P. Voskresenskii, A. S. Il'ina, and V. S. Tatarenchik, "Supersonic flow over wings with attached shock waves," Tr. Tsentr. Aéro-Gidrodin. Inst., No. 1950 (1974).
2. G. P. Voskresenskii, "Numerical solution of flow over an arbitrary surface of a triangular wing in the expanded supersonic region," Izv. Akad. Nauk SSSR. Mekh. Zhidk. Gaza, No. 4 (1968).
3. G. P. Voskresenskii, "Numerical solution of the flow over the top surface of a triangular wing in the expanded supersonic region," Zh. Prikl. Mekh. Tekh. Fiz., No. 6 (1973).
4. G. P. Voskresenskii, A. S. Il'ina, and V. S. Tatarenchik, Supersonic Flow over Wings, Institute of Applied Mathematics, Preprint 104 (1976).